REPORT

SP11 MERRIC

REMOTE IDENTIFICATION, CHARACTERIZATION AND MONITORING OF EROSIONAL PROCESSES

DOC.NO. 20170031-03-R
REV.NO. 0 / 2018-03-21

NORWEGIAN GEOTECHNICAL INSTITUTE
NGI.NO

Project

Project title:	SP11 MERRIC
Document title:	Remote Identification, Characterization and Monitoring of Erosional Processes
Document no.:	20170031-03-R
Date:	2018-03-21
Revision no. /rev. date:	0 /

Client

Client:	NGI / NFR
Client contact person:	Unni K. Eidsvig
Contract reference:	SP 11 GBV 2017

for NGI

Project manager:	Unni K. Eidsvig
Prepared by:	Sean E. Salazar, Anne Hormes, Dieter Issler
Reviewed by:	Regula Frauenfelder

NORWEGIAN GEOTECHNICAL INSTITUTE
NGI.NO

Main office
PO Box 3930 Ullevaal St.
NO-0806 Oslo
Norway

Trondheim office
PO Box 5687 Torgarden
NO-7485 Trondheim
Norway

T 22 02 30 00
F 22 23 04 48
NGI@ngi.no

BIC NO. DNBANOKK
IBAN NO26 5096 05 01281
ORGANISATION NO.
958 254 318MVA

ISO 9001/14001
CERTIFIED BY BSI
FS 32989/EMS 612006

Abstract

Remote sensing techniques and geophysical techniques have enabled the collection of vital information on geotechnical, hydrogeological, and environmental processes. These techniques may offer improvements over traditional data collection techniques or may provide data not readily available using conventional instrumentation. An assessment of various remote sensing and geophysical techniques, used to collect parameters of interest to the Multi-scale Erosion Risk under Climate Change (MERRIC) project, is provided in this technical note. This technical note is a deliverable of the MERRIC work package 4 on "Warning, monitoring, and non-physical mitigation measures".

A list of 11 key parameters for coastal erosion studies was established and matched with appropriate remote sensing techniques (including microwave, laser, and optical techniques) and on- and off-shore (or near-shore) geophysical techniques. The characteristics of each of the techniques is listed and background material is provided. The maturity of these techniques is described through examples in the literature and the potential for application within the scope of MERRIC is discussed. Many of the more mature techniques described in this technical note (for example, terrestrial lidar scanning [TLS], or electrical resistivity tomography [ERT]) are already routinely used in NGI projects, and thus, their relevance for MERRIC is well understood. Other emerging techniques (for example, terrestrial radar interferometry, or multi-beam echo sounding [MBES]) are less commonly applied, but may nonetheless prove to be indispensable for future projects related to MERRIC. It is, therefore, recommended that the potential of emergent remote sensing and geophysical techniques will be further investigated using the resources available at NGI.

Contents

Review and reference page

1 Introduction

The techniques that may be used to collect information about erosional processes, in the context of the MERRIC project, are discussed in this technical note. Specifically, remote sensing and geophysical techniques of interest are presented. The included techniques are not intended to be comprehensive; rather they are limited to established techniques that are expected to provide useful data for the identification, characterization, and continued monitoring of erosion phenomena.

In this Chapter 1, a general overview of remote sensing and geophysics is provided. In addition, a discussion of the applications of each of these approaches, within the scope of the MERRIC project, is included. Specifically, a table containing the parameters of interest for studying erosional processes is provided. Alongside each parameter of interest, proposed methods of collecting data, used to determine the parameter, is included. In Chapter 2, each of the proposed remote sensing and geophysical techniques are described in detail. Wherever possible, relevant examples or case studies from the literature are included for reference. Furthermore, resources available at NGI (e.g. equipment, etc.) are highlighted. In Chapter 3, limitations and recommendations for Work package 4 "Warning, monitoring, and non-physical mitigation measures" have been identified.

1.1 List of Acronyms

AEM	Airborne Electromagnetic Mapping
AGL	Above Ground Level
ALB	Airborne Lidar Bathymetry
CPT	Cone Penetration Test
CVES	Continous Vertical Electrical Sounding
DEM	Digital Elevation Model
DGPS	Differential GPS
DInSAR	Differential Interferometric Synthetic Aperture Radar
DSAS	Digital Shoreline Analysis System
DSLR	Digital Single Lens Reflex
EEARL	Experimental Advanced Airborne Research Lidar
ERT	Electrical Resistivity Tomography
ESA	European Space Agency
FEM	Frequency-domain Electromagnetic
GCP	Ground Control Points
GIS	Geographic Information Systems
GMTSAR	General Mapping Tool Synthetic Aperture Radar
GPR	Ground Penetrating Radar
GPRI	GAMMA Portable Radar Interferometer

GPS	Global Positioning System
InSAR	Interferometric Synthetic Aperture Radar
IP	Induced Polarization
IPTA	Interferometric Point Target Analysis
IRT	Infrared Thermography
LiDAR	Light Detection And Ranging (Commonly 'Lidar')
LOS	Line of Sight
LWIR	Long-wave Infrared
MBES	Multi-beam Echo Sounding
MERIS	Medium Resolution Imaging Spectrometer
MERRIC	Multi-scale Erosion Risk under Climate Change
MSS	Multi-spectral Scanner
MWIR	Mid-wave Infrared
NASA	National Aeronautics and Space Administration (United States)
NGI	Norwegian Geotechnical Institute
NIR	Near Infrared
OBIA	Object Based Image Analysis
PSI	Persistent Scatterer Interferometry
RaDAR	Radio Detection And Ranging (Commonly 'Radar')
RPAS	Remotely Piloted Aircraft System
RPS	Rotary Pressure Sounding
RTK-GNSS	Real-time Kinematic - Global Navigation Satellite System
SAR	Synthetic Aperture Radar
SBAS	Small Baseline Subset
SfM	Structure-from-Motion
SHOALS	Scanning Hydrographic Operational Airborne Lidar System
SMAP	Soil Moisture Active Passive
SMOS	Soil Moisture and Ocean Salinity
SPOT	Systeme Pour l'Observation de la Terre
SWIR	Short-wave Infrared
TEM	Time-domain Electromagnetic
TLS	Terrestrial Lidar (or Laser) Scanning
TM	Thematic Mapper
TRAR	Terrestrial Real Aperture Radar
USGS	United States Geological Survey
VLOS	Visual Line Of Sight
VTOL	Vertical Take Off and Landing
WP4	Work Package 4 (MERRIC Project)

1.2 Remote Sensing

The earliest modern developments of remote sensing techniques date back to the advent of military surveillance aircrafts, the launch of the first satellites into orbit, and the establishment of the Global Positioning System (GPS). Today, there are many types of sensors that are utilized, which are broadly categorized into active sensors and passive sensors. Active sensors emit radiation and measure the energy of the back-scattered radiation, whereas passive sensors rely only on reflected energy from an outside source (typically, the sun) or naturally emitted radiation (examples: photography, spectroradiometry). Furthermore, these sensors may be integrated into different platforms, such as spaceborne, airborne, or terrestrial platforms. Each sensor and platform combination possesses inherent strengths and weaknesses, making some combinations more suited to certain applications than others. For the remote sensing applications discussed in this technical note, the radiation wavelengths of interest are broadly illustrated by the chart presented in Figure 1.1.

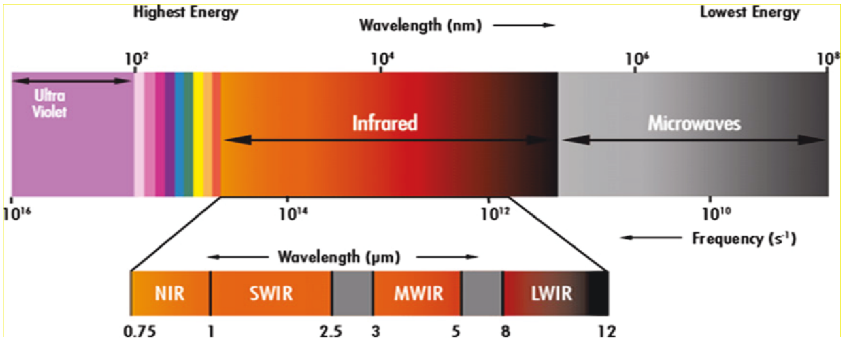

Figure 1.1. Wavelengths of the electromagnetic spectrum used for remote sensing applications (Figure source: Edmund Optics 2017).

1.2.1 Advantages

There are numerous advantages of remote sensing over traditional measurement techniques. These advantages are itemized as follows.

- Data are collected without being in contact with the area of interest (non-destructive).
- The amount and types of collectible data may be increased, allowing for more information to be captured.
- Spatial and temporal resolution may be greatly improved.
- Data may be collected and processed very quickly.
- Substantial cost savings may be realized, as compared to historical sampling methods.
- Remotely sensed data are collected from afar and may, therefore, be collected in areas that are hazardous or are otherwise inaccessible.

1.2.2 Platforms

Although there are now hundreds of satellites in Low Earth Orbit with many different types of sensors, there are still disadvantages to satellite-based (spaceborne) remote sensing. The most notable disadvantages include limited spatial resolution and temporal separation between passes. Furthermore, atmospheric conditions (cloud cover, smoke cover) may obscure or prevent the collection of clear imagery. Therefore, airborne and terrestrial platforms are also used to collect remote sensing data. The term 'proximal sensing' is sometimes used when describing data collection techniques that require relatively close proximity between the source of information and the sensor used to collect that information. Some of the geophysical and some of the remote sensing techniques described in this technical note may at times fall into this category, but for the purposes of this technical note, the data collection techniques are broadly classified as either 'remote sensing' or 'geophysical' techniques.

1.3 Geophysics

Geophysics is the application of physics to study geological material properties and subsurface phenomena in rock, soil, and water. Various geophysical techniques have been developed to relate subsurface conditions (e.g. electrical resistivity, or seismic wave velocity) to fundamental properties of the material in which these are measured (e.g. density, or porosity). The application of geophysical techniques, therefore, allows for the identification, classification, and evaluation of subsurface properties without having to physically retrieve and test samples. Furthermore, many geophysical techniques allow for the measurement of properties to considerable depths and over expansive areas in a relatively short amount of time. There are several platforms for the application of geophysical techniques, though most are performed *in situ* (i.e. in direct contact with the ground or body of water etc.) and, therefore, require the deployment of trained personnel to collect data.

1.4 Applications to MERRIC

The parameters of interest that have been identified – in collaboration with the other MERRIC work packages – for the modelling of erosional processes are presented in Table 1.1. The techniques that have been, or may be, applied to identify and to quantify these parameters by means of remote sensing or geophysical techniques (described in this technical note) are listed alongside the parameters in the table. Additionally, expected characteristics of the measurement techniques are described in terms of scale, resolution, accuracy, and implementation feasibility (within the different market areas at NGI). It should be noted that the characteristic values listed are highly variable and depend heavily on their specific applications. Therefore, ranges of values have been provided (where appropriate) for general reference. Each technique is described in more detail, alongside notable examples from the literature, in Chapter 2.

The proposed techniques have been applied to the study of a variety of erosion phenomena, such as coastal evolution (shoreline erosion and accretion), riverbank erosion, landslides, debris flows, and snow avalanches. It is proposed that a complementary and multi-scale approach that combines both geophysical and remote sensing methodologies is pursued to study these problems. Furthermore, data from these techniques should be integrated into geographic information systems (GIS) platforms for further analysis.

Table 1.1. Parameters of interest for modelling of erosional processes on- and offshore.

Parameter	Onshore/ Offshore	Measurement Technique	Scale	Resolution	Accuracy	Implementation Feasibility
Type of Sediment/Rock	Onshore	Hyperspectral imagery	varies	> 10 nm (λ)	1 nm (λ)	Mines, Miljø
		AEM	$10e^2$ - $10e^5$ m^2	m	m	Yes
	Offshore	Waterborne CVES/ERT	$10e^3$ - $10e^6$ m^2	1 - 10 m	m	Yes
		AEM	$10e^2$ - $10e^5$ m^2	m	m	Yes
Sediment Grain Size	Onshore	Photosieving	10 - 100 m^2	1 - 2 mm *†	$10e^{-2}$ mm	Naturfare, Miljø, BAS
	Offshore	Chirp sonar	$10e^3$ - $10e^6$ m^2	1 - 10 m	m	Possibly
Grain Size Distribution	Onshore	Photosieving	varies	1 - 2 mm *†	$10e^{-2}$ mm	Naturfare, Miljø, BAS
	Offshore	Chirp sonar	$10e^3$ - $10e^6$ m^2	1 - 10 m	m	Possibly
Sediment Bulk Density (Bed)	Onshore Offshore	AEM	$10e^2$ - $10e^5$ m^2	m	m	Yes
Bed Depth	Offshore	MBES Bathymetry	$10e^3$ - $10e^6$ m^2	m	m	Yes
		Waterborne CVES/ERT	$10e^3$ - $10e^6$ m^2	1 - 10 m	m	Yes
Susp. Sediment Concentration	Offshore	Spaceborne Optical	120-290 km swaths	10 m - 60 m	varies	Yes
		MBES Bathymetry	$10e^3$ - $10e^6$ m^2	1 - 10 m	m	Possibly
Thermal Gradient	Onshore	IRT	$10e^1$ - $10e^3$ m^2	cm - m *†	varies	Yes
Surface Roughness	Onshore	Photogrammetry	$10e^1$ - $10e^3$ m^2	cm - m *†	mm - cm	Yes
		Lidar	$10e^2$ - $10e^4$ m^2	cm - m *†	cm	Yes
Erosion Detection	Onshore	Photogrammetry	$10e^1$ - $10e^3$ m^2	cm - m *†	mm - cm	Yes
		Lidar	$10e^2$ - $10e^4$ m^2	cm - m *†	cm	Yes
		InSAR	20-400 km swaths	0.5 m - 100 m *	mm	Yes
		TRAR	$10e^2$ - $10e^5$ m^2	1 m - 10 m †	mm	Yes
	Offshore	MBES Bathymetry	$10e^3$ - $10e^6$ m^2	1 - 10 m	m	Yes
		Laser Bathymetry	$10e^3$ - $10e^6$ m^2	1 - 10 m	m	No
		Waterborne CVES/ERT	$10e^3$ - $10e^6$ m^2	1 - 10 m	m	Yes
Erosion Quantification	Onshore	Photogrammetry	$10e^1$ - $10e^3$ m^2	cm - m *†	mm - cm	Yes
		Lidar	$10e^2$ - $10e^4$ m^2	cm - m *†	cm	Yes
		InSAR	20-400 km swaths	0.5 m - 100 m *	mm	Yes
		TRAR	$10e^2$ - $10e^5$ m^2	1 m - 10 m †	mm	Yes
	Offshore	MBES Bathymetry	$10e^3$ - $10e^6$ m^2	1 - 10 m	1 - 10 m	Yes
		Laser Bathymetry	$10e^3$ - $10e^6$ m^2	1 - 10 m	1 - 10 m	No
		Waterborne CVES/ERT	$10e^3$ - $10e^6$ m^2	1 - 10 m	1 - 10 m	Yes
Subsidence/ Settlement	Onshore	InSAR	20-400 km swaths	0.5 m -100 m *	mm	Yes
		TRAR	$10e^2$ - $10e^5$ m^2	1 - 10 m †	mm	Yes

*sensor dependent
†range dependent

2 Measurement Techniques

2.1 Remote Sensing Techniques

2.1.1 Radar Remote Sensing

Spaceborne Radar

Synthetic Aperture Radar (SAR) sensors carried by satellites are utilized to emit and to gather microwave energy at various wavelengths and with various polarizations. Signals returned from the surface of the Earth, called backscatter, contain both phase and amplitude information. Phase information may be interpreted to generate digital elevation models (DEM) of surfaces while amplitude (or intensity) information may be used for classification purposes.

In a SAR technique called interferometric SAR (InSAR), phase information is further analysed to detect and measure line-of-sight deformation over time. For example, Aly et al. (2012) utilized an InSAR technique to study shoreline erosion and accretion, which occurred over a two-decade period, in the Nile Delta region in Egypt. Specifically, tandem coherence of the SAR data and an edge detection technique were utilized to detect changes in the boundary between water and land over time with high precision (Figure 2.1.). It was concluded that the application of InSAR was powerful, because it was possible to quantify the effectiveness of shoreline protection measures for a large coastline region.

Advanced, multi-temporal InSAR techniques include Persistent Scatterer Interferometry (PSI), a specific class of Differential InSAR (DInSAR). There are several unique algorithms that fall under the PSI umbrella, including the Small Baseline Subset (SBAS) approach, Interferometric Point Target Analysis (IPTA), SqueeSAR™ , and StaMPS. Each approach has advantages and disadvantages, depending on their application (e.g. urban vs. non-urban areas). Thorough reviews of the various PSI techniques available are included in Crosetto et al. (2016) and Osmanoğlu et al. (2016). Cigna et al. (2012), Wegmüller et al. (2012), Notti et al. (2014), Barra et al. (2016), and Casagli et al. (2017) all provide guidance on the state-of-the-art of PSI analysis techniques for detecting and quantifying landslide phenomena.

In some cases, a combination of techniques may be employed to improve a model of a phenomenon. For example, conventional differential InSAR and PSI techniques may be combined to improve spatial coverage over natural and uninhabited landscapes with less persistent scatterers (Kourkouli et al. 2014). In other instances, it may be beneficial to interpret both the phase and amplitude information for a given problem. For example, polarimetric moisture inversion techniques, such as the Small Perturbation Method and the Integral Equations Method, have been used to extract volumetric water content of soils through correlation with the apparent dielectric constant of the soil (Wagner 1998, Garner 2017). Although there are spaceborne sensors that use amplitude signals to extract soil moisture on the surface of the Earth, such as the European Space Agency's

(ESA) L-band Soil Moisture and Ocean Salinity (SMOS) mission (30-50 km resolution) or the partially defunct Soil Moisture Active Passive (SMAP) mission (9 km resolution) launched by the National Aeronautics and Space Administration (NASA), these missions were designed for large spatial coverage and, therefore, suffer in resolution. Wegmüller (1997) demonstrated that ERS SAR intensity images could be used for high resolution soil moisture monitoring in local areas and Barrett et al. (2009) provided a comprehensive review of the current techniques that are used to extract soil moisture from spaceborne radar remote sensors.

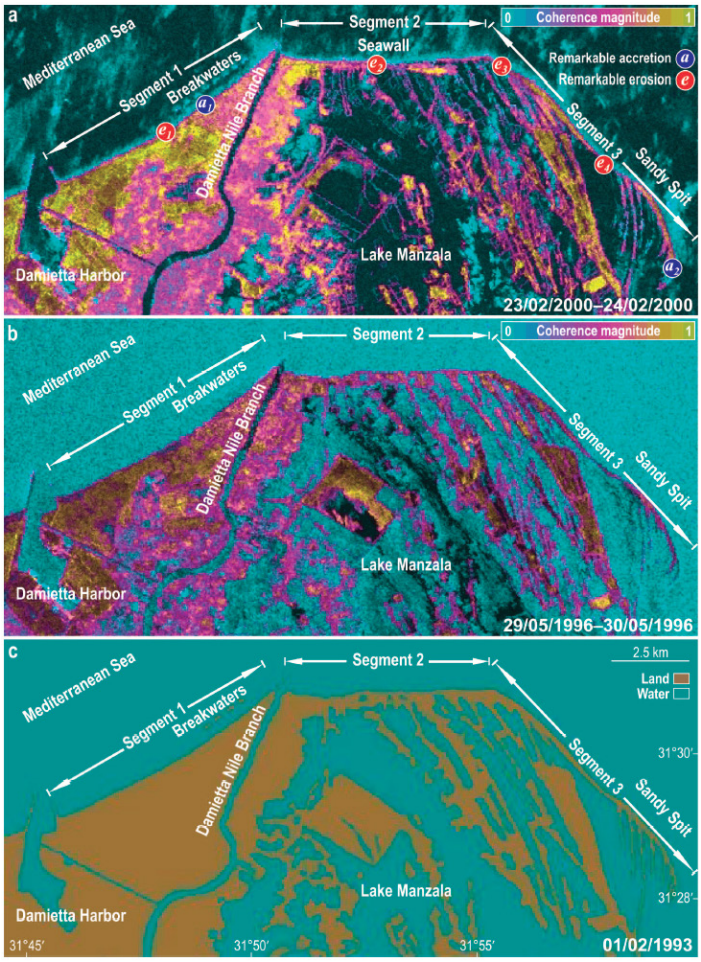

Figure 2.1. ERS SAR images were used for coherence and amplitude classification to identify the water/land boundary along a shoreline of the Damietta Promontory, Egypt (Figure source: from Aly et al. 2012).

Terrestrial Radar

Terrestrial radar interferometry is another form of radar remote sensing that has been deployed to study many anthropogenic and natural phenomena. Similar to InSAR techniques, terrestrial radar techniques utilize either a synthetic or real aperture to emit

and to collect coherent backscatter that is reflected from a target. Terrestrial platforms have been developed to allow for the collection of higher spatial and temporal resolution data with user-defined temporal resolution. A comprehensive review of terrestrial radar interferometry was provided by Caduff et al. (2015).

A terrestrial real aperture radar (TRAR) interferometry technique, utilizing the GAMMA Portable Radar Interferometer (GPRI) instrument, was employed in each of the following examples in the literature: Kos et al. (2011) and Rosenblad et al. (2016) characterized rock slope instability on steep faces; Caduff et al. (2013, 2014), Rosenblad et al. (2013), and Strozzi et al. (2015) studied slope deformation as a result of slow moving landslides; Wiesmann et al. (2015) and Caduff et al. (2016a, 2016b) studied snowpack displacement and snow avalanches. Other ground-based radar techniques have also been developed specifically for snow measurements (Ash et al. 2010, 2014, Vriend et al. 2013, Köhler et al. 2016).

The advantages of the terrestrial radar platform include user-controlled vantage points and incidence angles to maximize the effectiveness of detecting line of sight deformations and user-defined temporal resolution. Terrestrial observations are particularly well suited to monitoring fast-moving phenomena that could not be quantified with spaceborne SAR due to the time between satellite passes. A disadvantage of the terrestrial platform includes the need to physically collect data in the field (i.e. to pick vantage/reoccupation points carefully). Furthermore, geocoding the data requires high resolution digital elevation models (DEM) that may have to be collected by other means (e.g. lidar, photogrammetry).

WP4 Applications

Due to repeat pass observations of spaceborne radar sensors, InSAR techniques are particularly well suited for accurate characterization of slow moving phenomena, such as large-scale subsidence, localized settlement, or coastal erosion over time. However, InSAR and TRAR techniques have also been applied to study relatively fast moving erosional processes, such as landslides and snow avalanches.

Currently, spaceborne radar data is offered free of charge through the ESA Copernicus missions. The Sentinel-1 mission is a two-satellite constellation (1A and 1B) providing C-band SAR data following decommission of the ERS-2 (1995-2011) and Envisat (2002-2012) missions (Sentinel-1A launched in April 2014, Sentinel-1B launched in April 2016). Expected operational lifespan is 7 to 12 years and Level-1 data (Single Look Complex) in four modes with various swath widths and spatial resolutions are provided.

Currently, terrestrial radar data can be collected using the state-of-the-art TRAR instrument developed by e.g. GAMMA (instruments from other providers exist as well). NGI owns and operates one of these second generation GPRI instruments (Figure 2.2).

Figure 2.2. NGI engineers deploy the GAMMA Portable Radar Interferometer (GPRI) instrument to scan for line of sight deformation along a rock face.

2.1.2 Laser Remote Sensing

Terrestrial Lidar Scanning (TLS)

Terrestrial lidar (light detection and ranging) scanning is an effective scanning technology to capture landscape features and constructions in 3D with high accuracy and a very short collection time. The rapid development laser distance meters with a range of 2-3 km coupled with powerful data acquisition systems now offers a cheaper and simpler possibility for creating DEMs. Topographical lidar systems transmit light pulses in the near infrared (NIR) wavelength range (1064 nm typical) and calculate the duration between an emitted laser signal and the reflected returned signal. Time-o-flight laser scanners are typically used on long distances and precision is, among other factors, dependent on the accuracy of the internal clock that times the laser beam. Range accuracy for a long range lidar is typically within one centimeter. Time-of-flight lasers are ideal for measuring rock faces and snow covers at distances up to some kilometers. Phase based laser scanners are used at shorter range and have in general a much higher precision than time-of-flight laser scanners. Phase based scanners are mostly used for mapping manmade structures like buildings and industrial installations.

Lidar related services at NGI have been used for:

- Large scale landslide and rockfall mapping and monitoring
- Snow avalanche evaluation of failure area and path
- Volume calculation of: failure masses and unstable masses
- Building deformation monitoring and calculations during construction and renovation
- Data collection and processing for drill and blast tunneling:

- Discontinuity measurements
- CAD vs. actual
- Overbreak/underbreak
- Clearance
- Tunnel progression
- Water leakage into the tunnel
- Distribution and spacing of rock bolts
- Shotcrete thickness mapping and evaluation

At NGI's test site in Ryggfonn, a lidar located on Sætreskarsfjellet acquired a DEM with a horizontal resolution of about 2 m in the course of two hours. The sensor emits short pulses of near-infrared (NIR) light and measures the travel time. However, this method is not insensitive to the lighting conditions. Experience has shown that the presence of a thin skin of water on the snow grains on the surface can degrade the performance of the lidar due to strong absorption. Moreover, even a thin surficial ice crust can lead to deflection of direct or indirect sunlight to the receiver and drown the signal. Under poor weather conditions with fog, rain or snowfall, it is virtually impossible to obtain lidar measurements.

Laser Bathymetry

Highly specialized "green" lidar systems have been developed for near-shore bathymetric surveys. These systems typically transmit a blue-green wavelength laser (530 nm typical), so that they may penetrate shallow bodies of water, but may also transmit a second, near-infrared (NIR) wavelength laser (1064 nm or 1550 nm typical) for seamless profiles between subsurface and coastal terrain (Klemas 2011). The need for lidar bathymetry arose due to the ineffectiveness of other remote sensing techniques for mapping coastal regions (e.g. photogrammetric imaging) and as an alternative to waterborne geophysical techniques (e.g. echo-sounding). Commercial examples of this technology include the Hawk Eye II (Airborne Hydrography, Sweden), the Laser Airborne Depth Sounder (Tenix LADS Corporation, Australia), the Scanning Hydrographic Operational Airborne Lidar System (SHOALS) (Optech, Canada) (Kinzel et al. 2013), and the Experimental Advanced Airborne Research Lidar (EEARL). Limitations of the ALB technique include not being able to measure bathymetric profiles for very deep or very shallow waters, waters in the surf zone, or water with high turbidity. Furthermore, due to the rarity of ALB instruments and the airborne nature of these missions, their use is often reserved for government and military operations.

WP4 Applications

NGI conducts operational engineering work and research using two terrestrial lidar instruments: 1) A long-range lidar (Optech ILRIS-LR), and 2) a short-range lidar (FARO Focus 3D). The Optech ILRIS-LR scanner is a long range time-of-flight based scanner capable of generating data at distances over 3500 meters, however the speed of collection is limited to 10000 points per second. This technology is ideally suited for slope monitoring and evaluation (specifically landslide, rockfall and snow avalanches).

The FARO Focus is a high-speed phase based scanner that collects data at a speed of 1 million points per second, the range of equipment is however limited to 120 meters. This technology is ideal for construction and tunneling environments where data collection time is limited and objects of interest are generally situated near accessible scanning locations. The FARO scanner is also ideal for measurements and analyses of deformations and cracks in buildings.

2.1.3 Optical Remote Sensing

Spaceborne Sensing

In another form of remote sensing, wavelengths in the "optical" range of the electromagnetic spectrum are interpreted. These include the visible, near infrared (NIR), mid-wave infrared (MWIR), short-wave infrared (SWIR), and long-wave infrared (LWIR) bands (as presented previously in Figure 1.1). Multispectral sensors capable of collecting radiometric information in these bands have been designed for spaceborne platforms, such as the USGS/NASA Landsat missions and the ESA Copernicus missions. The Copernicus Sentinel family (introduced in Section 2.1.1) includes Sentinel-2, a constellation with high-resolution sensors designed for monitoring inland waterways and coastal areas (Sentinel-2A was launched in June, 2015 and Sentinel-2B was launched in March, 2017), and Sentinel-3, a constellation carrying instruments designed to measure sea surface topography and ocean and land surface temperature and colour (Sentinel-3A was launched in February, 2016 and Sentinel-3B is expected to launch sometime in 2018). The Sentinel missions have replaced the Medium Resolution Imaging Spectrometer (MERIS) sensor aboard ESA's Envisat satellite.

There are numerous examples in the literature where multispectral remote sensing was used to study erosion. For example, Mars and Houseknecht (2007) used Landsat thematic mapper (TM) data in combination with topographic maps to quantify coastal erosion along a segment of the Arctic coast in Alaska between 1955 and 2005 (Figure 2.3). In another example, El-Asmar and Hereher (2011) demonstrated that satellite images from the Landsat multi-spectral scanner (MSS) and TM, and the Systeme Pour l'Observation de la Terre (SPOT) sensors could be used to detect spatio-temporal changes in the coastal zone east of the Nile Delta between 1973 and 2007. In yet other examples, suspended sediment concentrations have been determined remotely in oceans and sewage discharges using Landsat-8 optical imagery and MERIS imagery. For example, Schild et al. (2017) used Landsat-8 imagery in combination with in situ measurements to quantify suspended sediment concentration in subglacial sediment plumes from tidewater glaciers in Svalbard.

There are several advantages to these spaceborne optical data. As with satellite-based radar sensing, data is collected routinely for many regions of the world without having to request specific data acquisitions. Furthermore, historic data are often available to study temporally vast processes. Among the disadvantages, are that optical imagery is highly susceptible to atmospheric conditions (e.g. cloud cover) and data acquisitions are limited by the repeat pass interval. Some phenomena (e.g. flooding events) are,

therefore, not easily studied during an event; rather, before and after comparisons and time-series analyses are necessary. Furthermore, the resolution of historic imagery is often limited.

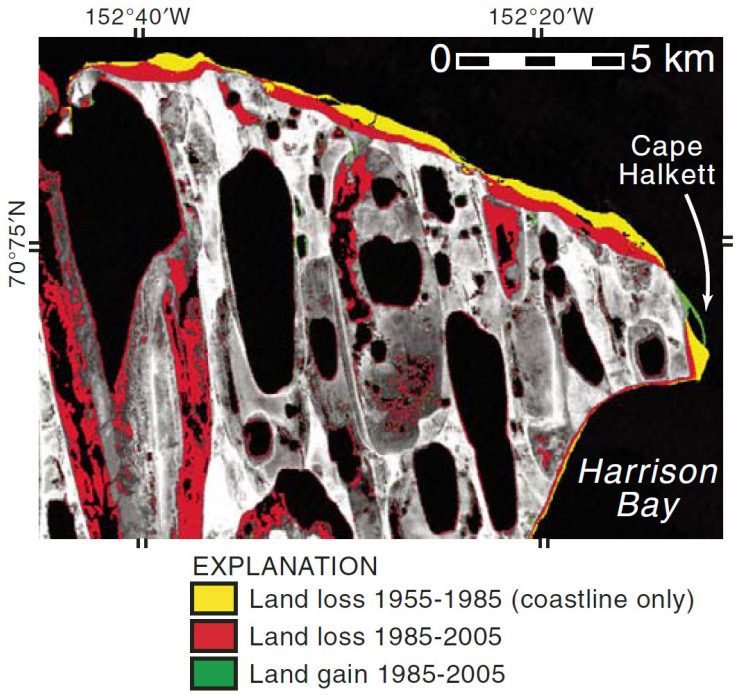

Figure 2.3. Landsat Thematic Mapper (TM) band 5 images were used to detect coastal erosion along the Beaufort Sea shoreline in Alaska (Figure source: modified from Mars and Houseknecht 2007).

Aerial Photogrammetry

Photogrammetric analysis of a set of images allows for the reconstruction of a DEM given a sufficient number of precisely known reference points that are visible in the images (in the previously mentioned case of alpine winter terrain, this is not a trivial matter). Comparison between DEMs created from images captured before and after an event (e.g. avalanche, debris flow) allow for the quantification of net volumetric erosion or deposition due to the event.

There have been published a variety of papers on the application of photogrammetry for soil erosion tracking and coastal erosion studies; a relatively early study e.g. by Brown and Arbogast (1999). More recent works are published by e.g. Catalão et al. (2005) and Heng et al. (2010). In snow avalanche research, photogrammetry has been used early on (Briukhanov et al. 1967), but the first application of this technique to the problem of snow erosion and deposition known to the authors is by Vallet et al. (2001), who surveyed an avalanche test site in Vallée de la Sionne in Switzerland. Images were collected from a helicopter immediately before and after artificial release of avalanches.

The technique was subsequently refined and routinely applied in several Vallée de la Sionne experiments (Sovilla 2004, Sovilla et al. 2006, 2010).

Although aerial photogrammetry has traditionally been collected from manned aircrafts, the recent proliferation of small, consumer-grade, remotely piloted aircraft systems (RPAS) and compact, high-resolution photography have provided more opportunity to collect imagery over large areas. RPAS-based remote sensing methods offer increasing accuracy, short acquisition times, and flexibility in hazardous or inaccessible areas, all at a relatively low cost (Scaioni et al. 2014). Due to the ability to "hover" in place with vertical-take-off-and-landing (VTOL) style RPAS, and the ideal vantage points that may be realized only with RPAS, aerial photography with RPAS is ideally suited to the investigation of erosional processes.

RPAS imagery combined with Structure-from-Motion (SfM) photogrammetric analyses may be used for repeated topographic surveys and, therefore, may be used to calculate erosion rates in any type of environment (Clapuyt et al. 2016). For example, Niethammer et al. (2012) and James et al. (2017a) demonstrated the effectiveness of deploying RPAS to collect high-resolution imagery of landslide structures. Ortho-mosaics and three-dimensional models were produced from the images allowing for measurements of the landslides that could be used in modelling. Similarly, Turner et al. (2015) used RPAS imagery to create a time-series of a landslide failure. Some further examples of RPAS-based SfM studies in the literature are summarized in Table 2.1. The characteristics of the RPAS missions and the accuracy of the results are also reported.

Table 2.1. Characteristics of RPAS-based photogrammetry reported in the literature.

Authors / Paper	RPAS	Image Overlap	Camera / Lens	Horiz. Precision	Vert. Precision	Ground Control Points	RTK-GNSS	Software	DEM Resolution
Turner et al. (2015)	Octocopter	60-80%	Canon EF-S 18–55 mm f/3.5–5.6 IS	21-76 cm	25-90 cm	23 GCP (2-4 cm accuracy)	No	Agisoft Photocscan	2 cm
Turner et al. (2014)	Octocopter	80-90%	Canon 18 mm f/3.5–f/5.6 IS	7 cm	6 cm	39 + 24 (DGPS meas.)	No	Agisoft Photocscan	5 m
Niethammer et al. (2012)	Quadrocopter		Praktica Luxmedia 8213	1-8.3 cm	4-6 cm	16 GCP (DGPS meas.)	No	OrthoVista	7-18 cm
Harwin & Lucieer (2012)	Octocopter	70-95%	DSLR with lens fixed at f/3.5	7.4 cm	7.4 cm	RTK GPS	Yes	PMVS2	1-3 cm
Clapuyt et al. (2016)	Octocopter	66-75%	Canon EF 50 mm f/1.8 II	40-61 cm	70 cm	15 GCP	No	VisualSFM	Varies
Nex & Remondino (2014)	Quadrocopter MD4-1000	Not reported	Olympus E-p1 17 mm nadir, 6 mm oblique	3.7 cm	2.3 cm	Total station meas. GCP	No	Various	Varies
Woodget & Austrums (2017)	Rotary-winged Draganflyer X6	Convergent overlap	Panasonic Lumix DMC-LX3	1-3 mm *	Not reported	25 GCPs	No	Agisoft Photoscan, CloudCompare	2 cm
James et al. (2017a)	Sirius 1 fixed-wing & Quadcopter		Panasonic Lumix GF1 & Praktica Luxmedia 8213	10 cm	10 cm	15 GCP & 122 GCP	No	Agisoft Photoscan	2.3 cm

* Accuracy dependent on processing method: 1 mm with point cloud roughness and 3 mm with image texture

Recent improvements in automated feature-matching algorithms (Micheletti et al. 2015) have allowed for the generation of dense three-dimensional point clouds that can be scaled and georectified to create DEMs (Westoby et al. 2012, Lucieer et al. 2013, Turner et al. 2014, James et al. 2017a, 2017b). Comprehensive reviews of RPAS deployment for remote sensing applications can be found in Colomina and Molina (2014), Nex and Remondino (2014), and Torresan et al. (2017).

The focus of continued developments in RPAS photogrammetry techniques is to increase the accuracy of surveys. Due to the time-consuming nature of locating individual Ground Control Points (GCP) with differential GPS (DGPS) measurements, efforts to develop on-board, real-time kinematic global navigation satellite systems (RTK-GNSS) have been made. In general, the accuracy of DEMs, derived from RPAS-based photogrammetry, depends on:

- Number of images collected
- Orientation of images
  - Distance from target
  - Amount of overlap
  - Stereo-angles
- Correct georectification
  - Number and density of GCP
  - Accuracy of GCP locations (often DGPS measured)
  - On-board RTK-GNSS capabilities
- Corrections made for lens distortions effects
- Camera sensor width, focal length, resolution

Based on industry trends over the last 5 years, it is expected that RPAS will continue to improve rapidly in the following areas: 1) resolution of sensors, 2) integration of more types of sensors, 3) flight-readiness and on-board navigation (RTK-GNSS, anti-collision sensors), and 4) flight duration (improved battery life). In addition to visible band imagery, there is also a great potential for RPAS-mounted infrared thermography (IRT) sensors (Klein 2016), as well as multi- and hyperspectral sensors (Jakob et al. 2017). IRT sensing could be used to detect thermal anomalies, indicating the presence of potential criticalities such as open fractures, scarps, moisture, and seepage zones. Multi- and hyperspectral sensing could be used to provide higher resolution supplements to data collected from spaceborne sensors.

One of the limitations on RPAS utilization today is flight regulations. Although these regulations differ somewhat from country to country, they are more or less similar in most Scandinavian and European countries. Examples of these flight regulations include visual line of sight (VLOS) requirements and restrictions concerning flight height above ground level (AGL). The flight regulations, therefore, demand careful mission planning and may limit some types of missions.

Photosieving

Surface sediment properties and the distribution of grain sizes in a topographic context are critical components to the study of processes such as flow resistance and erosion in flood, landslide, avalanche and coastal deposits. Furthermore, terrain and roughness are important parameters to understand sediment transport and erosion patterns and to predict flow velocities in open channels. The distribution of sediment deposition during avalanches, debris flows or flood events are key to site characterization. These processes also help gain a better understanding of the transport and deposition of toxic or environmentally hazardous material, such as heavy metals (Castillo-Lopez et al. 2017).

Traditional methods for determining sediment grain size distribution in the field are resource intensive. Furthermore, some characteristics, like bed roughness, have historically been measured with costly terrestrial laser scanning techniques (e.g. Entwistle and Fuller 2009). As an alternative, a method called photosieving has emerged. Photosieving utilizes photographs of deposit surfaces and automated image analysis to recognize grain size (Carbonneau et al. 2004, Castillo et al. 2011). Conventional aerial photographs have been used to classify particles from gravel to boulder size (coarser than 8 mm) (Butler et al. 2001). Airborne imagery has also been used to investigate suspended sediment and turbidity as well as bed sediments (Mertes et al. 1993, 2002, Castillo et al. 2011).

Flener (2015) pointed out that high-order hydrological models require increasingly higher resolution calibration data for geomorphology, roughness, and small scale river processes. Only recently have RPAS-based approaches provided such high resolution data, allowing for recognition of individual grains at the suprapixel level. For example, RPAS-based imagery with 4-6 cm ground resolution was collected over a 0.75 km^2 alluvial fan area (Carbonneau et al. 2012, De Haas et al. 2014). In another example, Tamminga et al. (2015, 2016) collected RPAS-based imagery with 5 cm ground resolution over a 1 km stretch of the Elbow River in Canada. It was shown that for 30 sample plots of 1 m^2 each, a statistical correlation with an R^2 value of 0.82 was achieved. In yet another example, Woodget and Austrums (2017) reported an accuracy of 0.1 mm for imagery collected over a riverbed in Cumbria, England.

A MATLAB-based algorithm called *BASEGRAIN* was developed by Detert and Weitbrecht (2012, 2013) at ETH Zurich and has been successfully tested in fluvial and glacial environments. The algorithm is based on the line-sampling method developed by Fehr (1987). The BASEGRAIN software produces grayscale images from original images and then grain areas are measured. Sampling sizes for BASEGRAIN are at least 150 grains with 30 grains in the medium grain-size fractions. In the original study, the accuracy of the grading curve based on image analysis was within 5 percent of the results obtained using classical dry sieving (Detert and Weitbrecht 2012). Westoby et al. (2015) compared results from photo-sieved grain-size distributions using BASEGRAIN 2.0 with a control dry-sieved distribution for sediments from a heterogeneous glacial moraine surface. The photo-sieved grain-size distribution deviated between 0.3 and 6.3

percent from the dry-sieving results. There are also other software algorithms available, including:

- An ArcGIS tool developed by Theler et al. (2008) to extract grain size distribution for debris flows.
- A QGIS plugin called GisedTrend, developed by Poizot and Méar (2010), that uses the Grain Size Trend Analysis (GSTA) method.

The primary advantage of the automated photosieving approach over traditional classification approaches is how rapidly sediments may be characterized at the site-scale. However, the approach is fundamentally limited by the quality of images used for analysis. Shadows, illumination conditions, camera focal length, particle size, and shot height are all factors that must be considered as part of the data collection procedure.

Photosieving Tests

BASEGRAIN 2.0 was tested by NGI staff for a set of RPAS-based images of a river plain in Utvik, Norway (Figure 2.4). In preliminary testing, it was determined that the software was not able to automatically identify grain sizes, due to the following reasons:

- RPAS flight height was 105 m AGL, which resulted in images with too coarse of a ground resolution for determining grain sizes.
- Lack of image scale to calibrate the length of grains/boulders and lack of resolution information (mm/pixel).
- Images used only had 96 dpi, but BASEGRAIN recommends at least 300 dpi images.

Additionally, manually captured images from a project in Flagstad (Norway) were tested. The images had a resolution of 22 mm/pixel, but problems were encountered with the size of the images. It is, therefore, recommended that a set of best practices are established that outline image resolution, flight height, etc. to ensure compatibility with analysis software. As an alternative to BASEGRAIN, a commercial software package called *eCognition* (by Trimble Inc.) may provide image analysis capability. eCognition uses object-based image analysis principles that could be adapted for classifying sediments in images. NGI currently possesses a license for eCognition and should, therefore, investigate the feasibility of using this software within the scope of the MERRIC project.

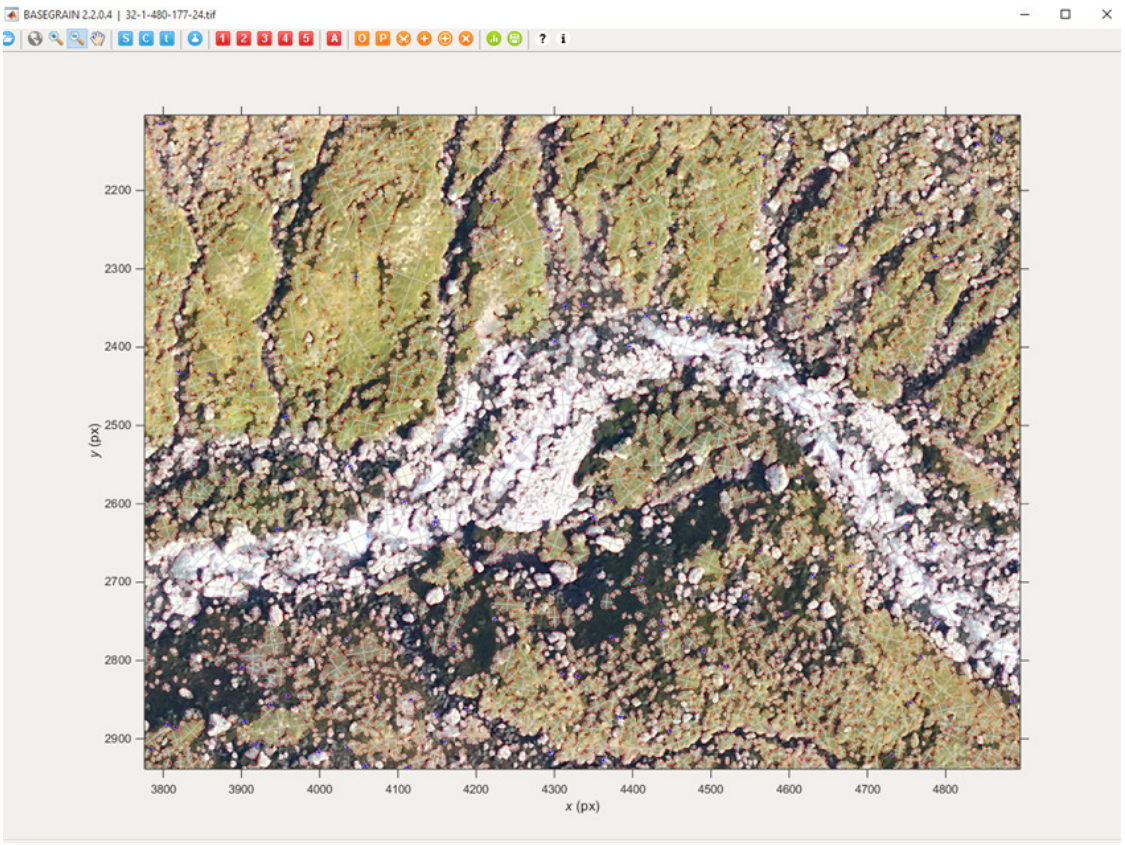

Figure 2.4. Example image from the Utvik site, tested with BASEGRAIN (coarse resolution and lack of scale rendered images unsuitable for photosieving with the software).

Gigapixel Photography

Gigapixel photography is a well-established and cost-effective method for producing high-resolution panoramic photographs. A GigaPan scanner is operated in conjunction with a DSLR camera and long-range lens to produce overlapping photographs, which are stitched together with software algorithms. This type of photography allows for extremely detailed visual inspection of large areas that cannot be achieved with any other type of visual remote sensor. Gigapixel photography is, therefore, a suitable tool for mapping rockfalls and unstable slopes, allowing engineers to virtually take the entire rock face back to the office to study it in detail. Depending on the size of the target, typical acquisition times for a panorama are between 10 and 30 minutes, allowing for rapid collection of data.

The correct processing workflow of gigapixel images is important for achieving good results. The individual, overlapping photos are post-processed to optimize highlights, shadows, and contrasts etc. During the post-processing and stitching, a pyramid data structure is built in order to facilitate fast and easy access to every part of the whole image. The finished product is uploaded to an online viewing platform (located at

www.gigapan.com) allowing engineers and clients direct and easy access from any web browser. An example of a finished GigaPan product is presented in Figure 2.5.

Rockfall hazard analyses at NGI are often carried out by combining the visual inspection benefits of gigapixel photographs with long-range LiDAR scanning. Data are acquired from the same position in order to better understand the three-dimensional structure of the target and to allow for distance and volume calculations.

Figure 2.5. Rock face in Svelvik, Norway (located behind NGI summer cabin) photographed with the gigapixel technique; with close up (inset) of an area of interest on the face.

2.2 Geophysical Techniques

2.2.1 Onshore Geophysical Techniques

Text sourced and modified from the NGI websites: https://www.ngi.no/eng/Services/Technical-expertise-A-Z/Geophysics-remote-sensing-and-GIS/ERT-IP, https://www.ngi.no/eng/Services/Technical-expertise-A-Z/Geophysics-remote-sensing-and-GIS/GPR, and https://www.ngi.no/eng/Services/Technical-expertise-A-Z/Geophysics-remote-sensing-and-GIS/AEM.

Electrical Resistivity Tomography (ERT)

Electrical Resistivity Tomography (ERT) is a near-surface geophysical method that uses direct current to measure the earth's resistivity. The current is injected into the subsurface through steel electrodes installed 10-20 cm into the ground and the apparent resistivity distribution along a profile or area is measured. Using data processing and inverse

modelling a two- or three-dimensional resistivity model of the subsurface can be derived.

Subsurface resistivity is highly variable and is mainly governed by the sediments and rock types (lithology) in the area. ERT thus enables us to distinguish different materials, ranging from low resistivity clay to high resistivity hard rock. A general estimate for depth of investigation is 10-20% of the array length, depending on the Earth resistivity structure. NGIs current instrument is capable of reaching a maximum depth of 70 m and an area of 400-1000 m can be conducted per day. NGI uses a combined ERT and time-domain IP system, an ABEM Terrameter LS (4 x 20 electrode cables, max array length 400m with 12-channel recording unit acquiring resistivity, IP windows and raw time series for advanced IP processing).

Geotechnical Applications:

- Bedrock depth/sediment mapping: In combination with boreholes or geo-technical logs (CPT, total soundings, RPS) the depth to bedrock can be mapped continuously and sedimentary infill distinguished.
- Quick clay: The salt content and thereby the conductivity of quick clay is normally lower than for non-sensitive clay. ERT can thus distinguish non-sensitive clay from sensitive clay.
- Geo-hazards/rock quality: Areas prone to rock slides are characterized by zones of fractured and incompetent rock. These zones are mostly clay and/or water-filled pockets detectable by ERT surveys.
- Archaeological artefacts: Old structures of timber, stones or bricks appear as small scale resistivity anomalies and can be distinguished if buried in highly conducting sediments, such as clay.
- Environmental risk assessment: With ERT, landfills can be mapped and delineated. In combination with Induced Polarization (IP), brownfield investigations, mineral prospection and groundwater-related issues can be conducted to characterize the subsurface contamination and its extent.

The data processing algorithms tend to poorly image sharp geological interfaces. Nevertheless, an ERT-inferred interface can be calibrated with just a few boreholes, and the total amount of required boreholes can be drastically reduced. Materials of similar resistivity (e.g. clay and shale) display a poor resolution and in case the subsurface and geology have an especially complex geometry, information based on one single profile may not be sufficient, and a grid of profiles or 3D surveying is recommended. Snow and ice are highly resistive. For this reason, it is in general recommended to undertake ERT fieldwork during warmer periods.

Ground Penetrating Radar (GPR)

GPR is based on sending high-frequency (typically several MHz up to a few GHz) electromagnetic waves into the ground and recording the strength and the time required for the return of any reflected signal. Reflections occur whenever the radar signal enters

into a material with different electrical conduction properties or dielectric permittivity from the material it left. The strength of the reflection is determined by the contrast in the dielectric constants and conductivities of the two materials. Very conductive material like clay and salt water attenuate the signal significantly and thus depth penetration will be very limited in these circumstances.

Higher frequencies allow better resolution but do not penetrate very deep whereas lower frequencies provide better depth penetration but less resolution. Thus, the choice of antenna frequency is crucial for best results. NGI equipment include: GSSI- SIR 4000 (central unit) and 200 MHz antenna. Antennae with different frequencies (from 16 MHz to 2.6 GHz) can be operated for targets outside the 200 MHz range. (http://www.geophysical.com/products.htm). NGI owns a step frequency radar (300 kHz to 3 GHz), developed and produced at NGI since 1989, and exported worldwide.

Applications of GPR include the determination of sediment conductivity (quick clay identification potential) bedrock depth, rock quality, detection of buried objects such as pipes an cables, archeological artefacts, subsurface layering, snow layering, void detection, non-destructive testing, investigation of contaminated ground, mapping of aquifers, identification of seepage zones in dam investigations.

Airborne Electromagnetic Mapping (AEM)

The AEM method (Figure 2.6) is based on the physical principles of electromagnetic induction. An electrical current is induced into the ground, creating a secondary magnetic field that measures the electrical resistivity of the ground. AEM systems measure the EM time decay or frequency response, and the related resistivity distribution is subsequently obtained by inverse modelling. We can differentiate Time-domain systems (TEM measuring EM step response decaying with time and frequency-domain systems (FEM) measuring continuously at several frequencies. TEM is well suited for deeper investigations due to the higher transmitter moment, while FEM tends to be superior for geology with high resistivity, maintaining high near- surface resolution. AEM data provide a powerful tool for geotechnical projects and planning of drillings due to coverage and survey speed. Based on the experience from three case studies, recommendations can be given for the setup of AEM-surveys for geotechnical projects:

- Drilling locations can be planned more efficiently based upon AEM results.
- Drilling results incorporated in AEM data interpretation and visualization lead to improved geological models (e.g. bedrock topography).
- AEM is better suited for regional-scale projects rather than isolated projects because costs are relatively high for small surveys. Parallel flight lines covering an area are preferable over flights which are aligned parallel to infrastructure long, linear infrastructure.
- Survey extent is limited by the presence of power lines and urban infrastructure.

The strengths of AEM can be summarised with the following characteristics:

- Efficiency AEM survey based on a proper feasibility study leads to substantial cost and resource reductions for ground investigations. AEM survey results deliver a regional overview of the geological complexity and, therefore, a strong asset and pre-condition for physical sampling.
- Accessibility Helicopter EM survey scan be carried out almost anywhere. High quality data can be obtained where factors such as vegetation, lakes, rivers, steep valleys, rugged terrain, and landowner permissions would limit ground accessibility. One of our most challenging and yet successful surveys so far was carried out at altitudes from 2,500 to 3,500 m above sea level in highly rugged terrain in the Himalayas. Imaging the geology under freshwater bodies (lakes, rivers or streams) poses no challenge, even salt water can be penetrated if shallower than about 30-40 m.
- Depth of penetration Base metal exploration has triggered development of powerful AEM systems that can penetrate hundreds of metres below the surface. Thus deep AEM soundings can be acquired easily, whereas most geophysical methods used for engineering applications is limited by some tens of metres.

Some examples of scenarios that are not suitable for AEM with today's state of the art include:

- Resolving sediment thickness thinner than 5 m;
- Mapping clay thickness over shale bedrock, as they tend to have the same resistivity.

Figure 2.6. Airborne Electromagnetic Mapping (AEM) technique deployed by NGI engineers at a site in Horten.

2.2.2 Offshore Geophysical Techniques

Multi-beam Echo Sounding (MBES)

The bathymetry of a river, a lake or the sea can be determined by sending pulses of (ultra-) sound from a transducer at a known location inside the water body vertically downward and measuring the time until the echo is received. This technique has been used for more than a century, having been first presented in a 1904 article in "Teknisk Ukeblad" by the Norwegian Hans Sundt Berggraf and patented in 1913 by the German

Alexander Behm. A decisive issue for the precision of the measurements is knowing the speed of sound in water, which is of the order of 1500 m s^{-1}, but depends strongly on the density, which in turn depends on salinity, temperature and depth. The speed increases by about 4 m s^{-1} for a temperature increase of 1 ºC in the most relevant range and by about 1 m s^{-1} for a salinity increase of 1%.

Echo sounding is largely non-invasive (the presence of the boat usually causes negligible disturbance of the flow field), yet requires extended cruises for covering large areas or obtaining bathymetry at high resolution. In order to monitor erosion/deposition at a few points, fixed sonar can be a good solution in many cases. When combined with acoustic Doppler current profilers, the measured erosion rates can be related to the flow conditions and thus the average shear stress.

In the last few decades, the technique has been developed further in many respects. Commercial devices are usually dual-frequency: The high-frequency channel (typically operating at 200 kHz) can operate to water depths of about 100 m. Due to the limited penetration depth of the sound waves, the bathymetry can be determined with good precision, but the reflecting layer might as well be dense vegetation or very soft mud. The low-frequency sound pulses (typically at 24 or 33 kHz) are partially reflected by the top boundary, but may partially penetrate more deeply and indicate at which depth a denser reflector is located.

An important development, initiated in the 1960s, but in wide-spread use only since the 1990s, is *swath bathymetry*. Thanks to special antennas, the emitted signal is relatively narrow in the direction of motion of the vessel (a few degrees), but wide (up to about 90 degrees) in the spanwise direction. A receiver antenna array allows the application of beam-forming techniques (i.e., echoes from different directions can be separated and the water depth determined across the entire swath at once). This allows strips about as wide as the water depth to be mapped at high resolution in one go.

The echo contains much more information than just the water depth. As mentioned above, if the frequency is low enough, the sound waves may penetrate the seafloor to some depth and be reflected at density horizons. Furthermore, density stratification, suspended sediment or fish in the water column may also reflect the sound waves. Algorithms have been developed to determine instantaneous sediment concentration distributions in a vertical plane (e.g. Simmons et al. 2010). Suspended particles are much smaller than the typical wavelength of the signals used by echo sounders. This leads to a very strong dependence $\sim (\lambda/d_p)^4$ of the scattering intensity, where λ is the wavelength of the signal and d_p is the diameter of the suspended particle. In order to determine the particle concentration from the reflected intensity, one, therefore, needs to know the mean particle size. In principle, one could determine the particle-size distribution and concentration by taking a large number of measurements at different frequencies, but in practice, one is probably always forced to take samples for calibration (Simmons et al. 2010).

Best et al. (2010) demonstrated that MBES data analysis can be carried even farther by looking at cross-correlations of the particle concentration between sweeps. In this way, the velocity field of the suspended particles (which essentially coincides with the velocity field of the water if the particles have low Stokes number) can be observed (Figure 2.7). It should be cautioned, however, that this method is still at the research and development stage.

As an example among a very large number of such studies, Chiang and Yu (2011) used bathymetry from echo-sounding together with seismic sections obtained with conventional air guns as the source and with chirp sonar devices to identify erosion processes along the Kaoping submarine canyon off south-western Taiwan. The imagery revealed multiple cut-and-fill features, deeply entrenched thalwegs, and sediment dispersal that were closely related to turbidity currents at the canyon head. However, such studies did not observe the erosion processes directly, but only their imprint from thousands to millions of years on the morphology and stratigraphy of the seafloor. Such data can be very valuable in validating numerical models of erosion and sediment transport, but since the flows were not directly observed, a number of assumptions were made.

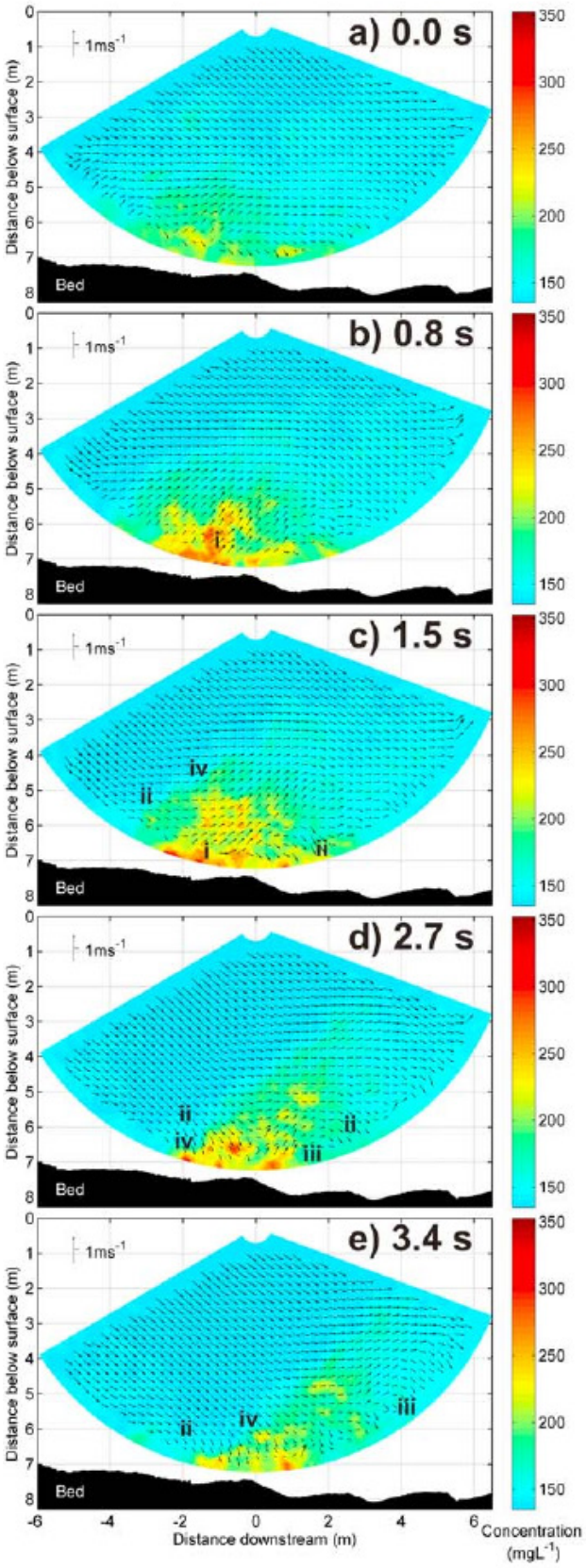

Figure 2.7. Time series of sediment concentration (color-coded) and flow-velocity fields (vectors) across the swath of a MBES. Flow is from left to right and vertical velocities are exaggerated by a factor of five (from Best et al. 2010).

Chirp Sonar

A recent development in the field of acoustic imaging applies rapid frequency sweeping during pulse emission to obtain profiles of acoustic impedance (Wang and Stewart 2015, and references therein). There are empirical relationships giving the acoustic impedance as a function of mean sediment grain size and sand content, which makes it possible to infer the subbottom composition from the chirp sonar data. A test of the chirp sonar method in a location where cores were available gave very encouraging results (Wang and Stewart 2015). In that case, chirps of 2 ms duration and sweeping in the range 2-10 kHz were used. For studying erosion, higher frequencies would improve distance resolution at the expense of penetration depth. The technique described by Wang and Stewart (2015) utilized only the acoustic impedance, but did not consider absorption. The inclusion of absorption might allow for the measurement of the sediment concentration in the flow as a function of particle size as well.

Waterborne Electrical Resistivity

An offshore, waterborne technique called continuous vertical electrical sounding (CVES) was utilized by Colombero et al. (2014) to reconstruct the sediment distribution of a lakebed down to a depth of 10 m. Crook and Rucker (2017) used a similar waterborne technique to survey a lakebed to depths of 35 m with shallow water depths (less than 20 m). For deeper parts of the lake, the streamer resistivity cables and electrode spacing had to be adapted.

2.3 Combination Techniques

In many cases, the combination of two or more measurement or analysis techniques may be necessary or desirable to provide a more complete picture of a given erosion phenomenon. Notable examples from the literature that utilized a combination of two or more remote sensing and geophysical techniques (discussed in this technical note) are provided as follows.

- Buckley et al. (2002), Buckley and Mitchell (2004), and Mills et al. (2005) proposed the fusion of data gathered from GPS, aerial photogrammetry, and InSAR techniques to create terrain models with improved quality over those models created with a single technique.
- Miller et al. (2008, 2009) used a surface matching technique to perform multi-temporal analysis of DEMs to assess geohazards in a dynamic coastal area in England. The technique overcame the lack of ground control, inherent to highly dynamic environments, by combining DEMs derived from photogrammetric analysis of historical airborne imagery and newly acquired, higher order DEMs derived from airborne lidar missions.
- Lague et al. (2013) provided a summary of the techniques that can be used to directly compare DEM point clouds that have been derived from multiple methods, such as terrestrial laser scanning and photogrammetry.

- Robson et al. (2015) combined optical, SAR, and topographic data to inventory, to outline and to monitor debris-covered glacier areas in the mountainous highlands of Nepal. This work was significant because it demonstrated the capabilities of these remote sensing technologies in a very challenging environment that is usually dominated by steep topography and loss of coherence between acquisitions due to snow and ice cover, and glacier movement.
- Prosdocimi et al. (2015) used SfM photogrammetry to study bank erosion for a network of agricultural drainage channels. DEMs that were created with photographs (captured from the ground) were compared with DEMs derived from high resolution terrestrial laser scanning. The erosion areas were effectively detected and deposition and erosion volumes were quantitatively estimated. This work was significant because it demonstrated that even simple, ground-based-photo campaigns combined with effective processing methods could produce accurate and immediately useful, quantitative results for pre- and post-erosion events.
- Thatcher et al. (2016) described the process of building topobathymetric elevation models as part of a national coastal elevation database in the United States. The project fused various techniques, including precision GPS, mobile terrestrial lidar, and high-resolution aerial photography to survey seawalls, artificial dunes, and topographic features in and around the interface between water and the urban landscape. In one pilot study area in the Outer Banks in North Carolina, the project collected up to 20 elevation datasets spanning the range from 1996 to 2012. Independent, lidar-derived DEMs were stacked to support time series analyses.
- Leyland et al. (2017) utilized a combination of mobile laser scanning, multibeam echo sounding (MBES), and acoustic Doppler current profiling techniques to directly measure river bank and bed changes and sediment flux.
- Thieler et al. (2017) developed an extensions to commercial Esri ArcGIS software, called the Digital Shoreline Analysis System (DSAS). The DSAS extension facilitates shoreline change calculations to provide rate-of-change and statistical information for reliability of results. In addition to historic shoreline mapping, DSAS may be utilized to calculate any positional change over time, such as river edge boundaries, or glacier movement.
- Confuorto et al. (2017) combined differential persistent scatterer interferometry analysis with geotechnical engineering analysis to study a slow moving, precipitation-induced landslide. It was concluded that by combining these analyses, a better understanding of the slope stability problem was achieved.
- Strozzi et al. (2007, 2013) and Caduff and Rieke-Zapp (2014) combined SAR analysis (DInSAR and PSI analyses) with aerial photogrammetry to inventory various landslides.
- Strozzi et al. (2015) combined SAR and TRAR techniques to measure slope deformations in the Canton of Valais, Switzerland. Data from various spaceborne radar sensors were combined with the terrestrial radar measurements to detect both slow and relatively rapid deformation phenomena.

3 Limitations and Recommendations

3.1 Limitations

- Although there is a multitude of remote sensing techniques with the capability to detect, map, and monitor erosion processes, measurements are limited to the terrain surface. Thus, studies are limited to erosional processes that can be detected from the surface. To study below-surface processes, geophysical techniques are required in addition/conjunction with remote sensing techniques.
- The lack of high temporal and spatial resolution data will limit historical analysis of some erosion sites. Data from current remote sensors will have to be fused with data from previous acquisitions for long-term monitoring.
- Although many of the proposed remote sensing and geophysical techniques can be utilized to provide input data for prediction models, the techniques are typically better suited to investigative studies and forensic analyses of existing, or ongoing erosion phenomena.
- Although there are free and open-source SAR processing software packages available (e.g. GMTSAR), this software may lack many of the advanced analysis tools of commercial software packages (e.g. GAMMA). Further parallel study is required to compare results.

3.2 Recommendations

- The most cost-effective remote sensing solutions for studying and quantifying erosion will likely be site-specific. Existing databases should be searched to obtain data that has already been collected.
- NGI already owns and operates a terrestrial radar instrument (GPRI) that should be utilized. Data reduction and interpretation will be performed in-house.
- The cost-effectiveness of deploying RPAS to survey a site should not be overlooked. The deployment of lidar is expected to be less cost effective than utilizing RPAS-acquired imagery. NGI already owns and operates multiple VTOL-style RPAS that should be utilized for photogrammetric surveys. Data reduction and interpretation will be performed in-house.
- Multi-temporal, non-technique/platform specific DEMs may be compared and updated using free and open-source software (e.g. Cloud Compare 2017).
- Although it is often difficult to directly interpret or combine remotely sensed data in the context of geotechnical engineering modelling and analysis, the various types of data that can be collected using remote sensing techniques should add value to stakeholders by allowing for a more complete picture of a problem.
- The applicability of many of the techniques presented in this technical note should be considered for the hydroelectric energy sector in Norway. The impact of erosional processes upstream, in reservoirs, and downstream may be of concern. For example, unusually large precipitation events in combination with

high meltwater activity could lead to increased water release, downstream erosion, or may induce rapid drawdown conditions on reservoir banks.
- It is good practice to validate (ground-truth) remotely sensed data whenever possible, especially when erroneous findings are suspected.

Acknowledgements

This material is based upon work supported by the National Science Foundation Graduate Research Fellowship Program under Grant No. DGE-1450079 and an international travel allowance through the Graduate Research Opportunities Worldwide (GROW) program, as awarded to S.E. Salazar. In connection with the GROW award, support has also been received by the Research Council of Norway. Any opinions, findings, and conclusions or recommendations expressed in this material are those of the authors and do not necessarily reflect the views of the National Science Foundation.

References

Agisoft, LLC (2017). *PhotoScan Professional (Version 1.3.4)*. 3D Measurements and Photogrammetric Modeling Software." St. Petersburg, Russia.

Aly, M.H., Giardino, J.R., Klein, A.G., and Zebker, H.A. (2012). "InSAR Study of Shoreline Change along the Damietta Promontory, Egypt." *Journal of Coastal Research*, Vol. 28, No. 5, pp. 1263–1269.

Ash, M., Brennan, P.V., Keylock, C.J., Vriend, N.M., McElwaine, J.N., and Sovilla, B. (2014). "Two-dimensional Radar Imaging of Flowing Avalanches." *Cold Regions Science and Technology*, Vol. 102, pp. 41-51. doi:10.1016/j.coldregions.2014.02.004.

Ash, M., Chetty, K., Brennan, P., McElwaine, J. & Keylock, C. (2010). "FMCW Radar Imaging of Avalanche-like Snow Movements." *Proceedings 2010 IEEE Radar Conference*, Washington, DC, USA. doi:10.1109/RADAR.2010.5494643.

Barra, A., Monserrat, O., Mazzanti, P., Esposito, C., Crosetto, M., and Mugnozza, S.G. (2016). "First Insights on the Potential of Sentinel-1 for Landslides Detection." *Geomatics, Natural Hazards and Risk*, Vol. 7, No. 6, pp. 1874–1883.

Barrett, B.W., Dwyer, E., and Whelan, P. (2009). "Soil Moisture Retrieval from Active Spaceborne Microwave Observations: An Evaluation of Current Techniques." *Remote Sensing*, Vol. 1, pp. 210-242. doi:10.3390/rs1030210.

Best, J., Simmons, S., Parsons, D., Oberg, K., Czuba, J., and Malzone, C. (2010). "A New Methodology for the Quantitative Visualization of Coherent Flow Structures in Alluvial Channels Using Multibeam Echo-Sounding (MBES). *Geophysical Research Letters*, Vol. 37, No. 6. doi:10.1029/2009GL041852.

Briukhanov, A.V., Grigorian, S.S., Miagkov, S.M., Plam, M.Y., Shurova, I.Y., Eglit, M.E., and Yakimov, Y.L. (1967). "On Some New Approaches to the Dynamics of Snow Avalanches." In: *Physics of Snow and Ice*, H. Ôura (Ed.), *Proceedings International Conference on Low Temperature Science 1966*, Sapporo, Japan, Vol. I, Part 2, pp. 1223–1241.

Brown, D., Arbogast, A. (1999). "Digital Photogrammetric Change Analysis as Applied to Active Coastal Dunes in Michigan", *Photogrammetric Engineering and Remote Sensing*, 65(4), 467–474.

Buckley, S.J., Mills, J.P., Clarke, P.J., Edwards, S.J., Pethick, J., and Mitchell, H.L. (2002). "Synergy of GPS, Photogrammetry and InSAR for Coastal Zone Monitoring." *Proceedings 7th International Conference on Remote Sensing for*

Marine and Coastal Environments, Miami, Florida, USA.

Buckley, S.J. and Mitchell, H.L. (2004). "Integration, Validation, and Point Spacing Optimisation of Digital Elevation Models." *The Photogrammetric Record*, Vol. 19, No. 108, pp. 277-295. doi:10.1111/j.0031-868X.2004.00287.x.

Butler J.B., Lane, S.N., Chandler, J.H. (2001). "Automated Extraction of Grain-Size Data from Gravel Surfaces Using Digital Image Processing." *Journal of Hydraulic Research*, Vol. 39, No. 5, pp. 519–529.

Caduff, R., Kos, A., Schlunegger, F., McArdell, B., and Wiesmann, A. (2014). "Terrestrial Radar Interferometric Measurement of Hillslope Deformation and Atmospheric Disturbances in the Illgraben Debris-flow Catchment, Switzerland." *Geoscience and Remote Sensing Letters*, Vol. 11, pp. 434–438. doi:10.1109/LGRS.2013.2264564.

Caduff, R. and Rieke-Zapp, D. (2014). "Registration and Visualization of Deformation Maps from Terrestrial Radar-Interferometry Using Photogrammetry and Structure from Motion." *The Photogrammetric Record*, Vol. 29, pp. 167–186. doi:10.1111/phor.12058.

Caduff, R., Schlunegger, F., Kos, A., and Wiesmann, A. (2015). "A Review of Terrestrial Radar Interferometry for Measuring Surface Change in the Geosciences." *Earth Surface Processes and Landforms*, Vol. 40, pp. 208–228. doi:10.1002/esp.3656.

Caduff, R., Strozzi, T., and Wiesmann, A. (2013). "Erfolgreicher Einsatz Terrestrischer Radar-Interferometrie zur flächenhaften Vermessung von ausserordentlichen Hangrutschungsbewegungen im Gebiet Hintergraben/OW." *Swiss Bulletin für Angewandte Geologie*, Vol. 18, pp. 129–138.

Caduff, R., Wiesmann, A., Bühler, Y., Bieler, C., and Limpach, P. (2016b). "Terrestrial Radar Interferometry for Snow Glide Activity Monitoring and its Potential as Precursor of Wet-Snow Avalanches." *INTERPRAEVENT 2016*, May 30 - 2 June, Lucerne, Switzerland.

Caduff, R., Wiesmann, A., Bühler, Y., and Pielmeier, C. (2016a). "Continuous Monitoring of Snowpack Displacement at High Spatial and Temporal Resolution with Terrestrial Radar Interferometry." *Geophysical Research Letters*, Vol. 42, pp. 813-820. doi:10.1002/2014GL062442.

Carbonneau, P.E., Lane, S.N., Bergeron, N.E. (2004). "Catchment-Scale Mapping of Surface Grain Size in Gravel Bed Rivers Using Airborne Digital Imagery." *Water Resource Research*, Vol. 40, No. 7, 11 pgs. doi:10.1029/2003WR002759.

Catalão, J., Catita, C., Miranda, J., Dias, J. (2002). "Photogrammetric analysis of the coastal erosion in the Algarve (Portugal)", Géomorphologie: relief, processus, environnement, 8-2; pp. 119–126.

Casagli, N., Tofani, V., Morelli, S., Frodella, W., Ciampalini, A., Raspini, F., and Intrieri, E. (2017). "Remote Sensing Techniques in Landslide Mapping and Monitoring, Keynote Lecture." *Proc. 4th World Landslide Forum*, Ljubljana, Slovenia, 19 pgs. doi:10.1007/978-3-319-53487-9_1.

Castillo, E., Pereda, R., Manuel de Luis, J., Medina, R., and Viguri, J. (2011). "Sediment Grain Size Estimation Using Airborne Remote Sensing, Field Sampling, and Robust Statistic." *Environmental Monitoring and Assessment*, Vol. 181, pp. 431–444. doi:10.1007/s10661-010-1839-z.

Castillo-Lopez, E., Pereda, R., Manuel de Luis, J., Perez, R., Pina, F. (2017). "Heavy Metals Estimation in Coastal Areas Using Remote Sensing, Field Sampling and Classical and Robust Statistic." *International Journal of Environmental, Chemical, Ecological, Geological and Geophysical Engineering*, Vol. 11, No. 9, pp. 794–798.

Chiang, C.S. and Yu, H.S. (2011). "Sedimentary Erosive Processes and Sediment Dispersal in Kaoping Submarine Canyon." *Science China Earth Sciences*, Vol. 54, No. 2, pp. 259–271. doi:10.1007/s11430-010-4076-y.

Cigna, F., Bianchini, S., and Casagli, N. (2012). "How to Assess Landslide Activity and Intensity with Persistent Scatterer Interferometry (PSI): the PSI-based Matrix Approach." *Landslides*, Vol. 10, pp. 267-283. doi:10.1007/s10346-012-0335-7.

Clapuyt, F., Vanacker, V., & Van Oost, K. (2016). "Reproducibility of UAV-based Earth Topography Reconstructions based on Structure-from-Motion Algorithms." *Geomorphology*, 260, pp. 4–15.

Cloud Compare (2017). *Cloud Compare (Version 2.9)*. Open Source 3D Point Cloud And Mesh Processing Software. Retrieved from http://www.cloudcompare.org.

Colombero, C., Comina, C., Gianotti, F., and Sambuelli, L. (2014). "Waterborne and On-land Electrical Surveys to Suggest the Geological Evolution of a Glacial Lake in NW Italy." *Journal of Applied Geophysics*, Vol. 105, pp. 191–202. doi:10.1016/j.jappgeo.2014.03.020.

Colomina, I. and Molina, P., 2014, "Unmanned Aerial Systems for Photogrammetry and Remote Sensing: A Review." *ISPRS Journal of Photogrammetry and Remote Sensing*, Vol. 92, pp. 79–97.

Confuorto, P., Martire, D.D., Centolanza, G., Iglesias, R., Mallorqui, J.J., Novellino, A., Plank, S., Ramondini, M., Thuro, K., and Calcaterra, D. (2017). "Post-failure Evolution Analysis of a Rainfall-triggered Landslide by Multi-temporal Interferometry SAR Approaches Integrated with Geotechnical Analysis." *Remote Sensing of Environment*, Vol. 188, pp. 51–72. doi:10.1016/j.rse.2016.11.002.

Crook, N., and Rucker, D.F. (2017). "Waterborne Electrical Resistivity of the Hypersaline Mono Lake." *Journal of Environmental and Engineering Geophysics*, Vol. 22, No. 2, pp. 191-196. doi:10.2113/JEEG22.2.191.

Crosetto, M., Monserrat, O., Cuevas-González, M., Devanthéry, N., and Crippa, B. (2016). "Persistent Scatterer Interferometry: A Review." *ISPRS Journal of Photogrammetry and Remote Sensing*, Vol. 115, pp. 78–89. doi:10.1016/j.isprsjprs.2015.10.011.

De Haas, T., Ventra, D., Carbonneau, P., Kleinhans, M.G. (2014). "Debris Flow Dominance of Alluvial Fans Masked by Runoff Reworking and Weathering." *Geomorphology*, Vol. 217, pp. 165–181.

Detert, M. and Weitbrecht, V. (2012). "Automatic Object Detection to Analyze the Geometry of Gravel Grains - A Free Stand-Alone Tool." *River Flow 2012,* R.M. Muños (Ed.), Taylor & Francis Group, London, ISBN 978-0-415-62129-8, pp. 595–600.

Detert, M. and Weitbrecht, V. (2013). "User Guide to Gravelometric Image Analysis by BASEGRAIN." In: *Advances in Science and Research*, S. Fukuoka, H. Nakagawa, T. Sumi, H. Zhang (Eds.), Taylor & Francis Group, London, ISBN 978-1-138-00062-9, pp. 1789–1795.

El-Asmar, H.M., and Hereher, M.E. (2011). "Change Detection of the Coastal Zone East Of the Nile Delta Using Remote Sensing." *Environmental Earth Sciences*, Vol. 62, No. 4, pp. 769-777. doi:10.1007/s12665-010-0564-9.

Entwistle, N.S. and Fuller, I.C. (2009). "Terrestrial Laser Scanning to Derive Surface Grain Size Facies Character of Gravel Bars." In: *Laser Scanning for the Environmental Sciences*, G.L. Heritage and A.R.G. Large (Eds.), Wiley-Blackwell, Oxford, UK, Chapter 7. doi:10.1002/9781444311952.ch7.

Fehr, R. (1987). "Einfache Bestimmung der Korngrössenverteilung von Geschiebematerial mit Hilfe der Linienzahlanalyse (Simple Detection of Grain Size Distribution of Sediment Material Using Line-Count Analysis)." *Schweizer Ingenieur und Architekt*, Vol. 105, pp. 1104–1109.

Flener, C. (2015). "Remote Sensing for Three-Dimensional Modelling of Hydromorphology." PhD dissertation, Turku University, Turku, Finland.

Garner, C.D. (2017). "Development of a Multiband Remote Sensing System for Determination of Unsaturated Soil Properties." PhD dissertation. University of Arkansas, Fayetteville, Arkansas, USA.

Graham, D.J., Reid, I., Rice, S.P. (2005a). "Automated Sizing of Coarse Grained Sediments: Image-Processing Procedures." *Mathematical Geology,* Vol. 37, No. 1, pp. 1–28.

Graham, D.J., Rice, S.P. and Reid, I. (2005b). "A Transferable Method for the Automated Grain Sizing of River Gravels." *Water Resources Research,* Vol. 41, No. 7, W07020. doi:10.1029/2004WR003868.

Harwin, S., and Lucieer, A. (2012). "Assessing the Accuracy of Georeferenced Point

Clouds Produced via Multi-view Stereopsis from Unmanned Aerial Vehicle (UAV) Imagery." *Remote Sensing*, Vol. 4, No. 6, pp. 1573–1599.

Heng, P., Chandler, J., Armstrong, A. (2010). "Applying close range digital photogrammetry in soil erosion studies", *The Photogrammetric Record*, https://doi.org/10.1111/j.1477-9730.2010.00584.x.

Jakob, S., Zimmermann, R., and Gloaguen, R. (2017). "The Need for Accurate Geometric and Radiometric Corrections of Drone-Borne Hyperspectral Data for Mineral Exploration: MEPHySTo - A Toolbox for Pre-Processing Drone-Borne Hyperspectral Data." *Remote Sensing*, Vol. 9, No. 88, pp. 1–17. doi:10.3390/rs9010088.

James, M.R., Robson, S., d'Oleire-Oltmanns, S., and Niethammer, U. (2017a). "Optimizing UAV Topographic Surveys Processed with Structure-from-Motion: Ground Control Quality, Quantity and bundle adjustment." *Geomorphology*, Vol. 280, pp. 51-66. doi:10.1016/j.geomorph.2016.11.021.

James, M.R., Robson, S., and Smith, M.W. (2017b). "3-D Uncertainty-Based Topographic Change Detection with Structure-from-Motion Photogrammetry: Precision Maps for Ground Control and Directly Georeferenced Surveys." *Earth Surface Processes and Landforms*, Vol. 42, No. 12, pp. 1769–1788. doi:10.1002/esp.4125.

Kinzel, P.J., Legleiter, C.J., and Nelson, J.M. (2013). "Mapping River Bathymetry with A Small Footprint Green Lidar: Applications and Challenges." *Journal of the American Water Resources Association*, Vol. 49, No. 1, pp. 183–204. doi:10.1111/jawr.12008.

Klemas, V. (2011). "Beach Profiling and LIDAR Bathymetry: An Overview with Case Studies." *Journal of Coastal Research*, Vol. 27, No. 6, pp. 1019–1028. doi:10.2112/JCOASTRES-D-11-00017.1.

Klein, M. (2016). "Photogrammetric Processing from Unmanned Aerial System (UAS) Data: Elephant Butte Dam." Technical Memorandum No. 8530-2016-28, Research and Development Office (Science and Technology Program), Bureau of Reclamation, U.S. Department of the Interior, 44 pgs.

Köhler, A., McElwaine, J.N., Sovilla, B., Ash, M., and Brennan, P. (2016). "The Dynamics of Surges in the 3 February 2015 Avalanches in Vallée de la Sionne." *Journal of Geophysical Research: Earth Surface*, Vol. 121, No. 11, pp. 2192–2210. doi:10.1002/2016JF003887.

Kos, A., Strozzi, T., Stockmann, R., Wiesmann, A., and Werner, C. (2011). "Detection And Characterization of Rock Slope Instabilities Using a Portable Radar Interferometer (GPRI)." *Proceedings 2nd World Landslide Forum*, Rome, Italy.

Kourkouli, P., Wegmüller, U., Teatini, P., Tosi, L., Strozzi, T., Wiesmann, A., and Tansey, K. (2014). "Ground Deformation Monitoring Over Venice Lagoon Using Combined DInSAR/PSI Techniques." *Engineering Geology for Society and Territory*, Vol. 4, pp. 183-186. doi:10.1007/978-3-319-08660-6_35.

Lague, D., Brodu, N., Leroux, J. (2013). "Accurate 3D Comparison of Complex Topography with Terrestrial Laser Scanner: Application to the Rangitikei Canyon (N-Z)." *ISPRS Journal of Photogrammetry and Remote Sensing*, Vol. 82, pp. 10-26. doi:10.1016/j.isprsjprs.2013.04.009.

Leyland, J., Hackney, C.R., Darby, S.E., Parsons, D.R., Best, J.L., Nicholas, A.P., Aalto, R., and Lague, D. (2017). "Extreme Flood-driven Fluvial Bank Erosion And Sediment Loads: Direct Process Measurements Using Integrated Mobile Laser Scanning (MLS) and Hydro-acoustic Techniques." *Earth Surface Processes and Landforms*, Vol. 42, No. 2, pp. 334-346. doi:10.1002/esp.4078.

Lucieer, A., Jong, S. M. D., and Turner, D. (2014). "Mapping Landslide Displacements Using Structure from Motion (SfM) and Image Correlation of Multi-temporal UAV Photography." *Progress in Physical Geography*, Vol. 38, No. 1, pp. 97–116.

Mars, J.C. and Houseknecht, D.W. (2007). "Quantitative Remote Sensing Study Indicates Doubling of Coastal Erosion Rate in Past 50 yr along a Segment of the Arctic Coast of Alaska." *Geology*, Vol. 35, No. 7, pp. 583–586.

Mertes, L.A., Smith, M.O., Adams, J.B. (1993). "Estimating Suspended Sediment

Concentrations in Surface Waters of the Amazon River Wetlands from Landsat Images." *Remote Sensing of Environment*, Vol. 43, No. 3, pp. 281–301.

Micheletti, N., Chandler, J.H., and Lane, S.N. (2015). "Structure from Motion (SfM) Photogrammetry." In: *Geomorphological Techniques (Online Edition)*, L.E. Clarke and J.M. Nield (Eds.), British Society for Geomorphology, London, ISSN 2047-0371, Chapter 2, Section 2.2.

Miller, P., Mills, J., Edwards, S., Bryan, P., Marsh, S., Mitchell, H., and Hobbs, P. (2008). "A Robust Surface Matching Technique for Coastal Geohazard Assessment and Management." *ISPRS Journal of Photogrammetry and Remote Sensing*, Vol. 63, pp. 529–542. doi:10.1016/j.isprsjprs.2008.02.003.

Miller, P., Mills, J., Edwards, S., Bryan, P., Marsh, S., Mitchell, H., and Hobbs, P. (2009). "Erratum to: 'A Robust Surface Matching Technique for Coastal Geohazard Assessment and Management." *ISPRS Journal of Photogrammetry and Remote Sensing*, Vol. 64, pp. 529–542. doi:10.1016/j.isprsjprs.2008.11.001.

Mills, J.P., Buckley, S.J., Mitchell, H.L., Clarke, P.J., and Edwards, S.J. (2005). "A Geomatics Data Integration Technique for Coastal Change Monitoring." *Earth Surface Processes and Landforms*, Vol. 30, No. 6, pp. 651–664. doi:10.1002/esp.1165.

Nex, F., and Remondino, F. (2014). "UAV for 3D Mapping Applications: A Review." *Applied Geomatics*, Vol. 6, No. 1, pp. 1–15.

Niethammer, U., James, M. R., Rothmund, S., Travelletti, J., and Joswig, M. (2012). "UAV-based Remote Sensing of the Super-Sauze Landslide: Evaluation and Results." *Engineering Geology*, Vol. 128, pp. 2–11.

Notti, D., Herrera, G., Bianchini, S., Meisina, C., García-Davalillo, J.C., and Zucca, F. (2014). "A Methodology for Improving Landslide PSI Data Analysis." *International Journal of Remote Sensing*, Vol. 35, No. 6, pp. 2186–2214.

Osmanoğlu, B., Sunar, F., Wdowinski, S., and Cabral-Cano, E. (2016). "Time Series Analysis of InSAR Data: Methods and Trends." *ISPRS Journal of Photogrammetry and Remote Sensing*, Vol. 155, pp. 90–102. doi:10.1016/j.isprsjprs.2015.10.003.

Poizot, E. and Méar, Y. (2010). "Using a GIS to Enhance Grain Size Trend Analysis." *Environmental Modelling & Software*, Vol. 25, No. 4, pp. 513–525.

Prosdocimi, M., Calligaro, S., Sofia, G., Dalla Fontana, G., and Tarolli, P. (2015). "Bank Erosion in Agricultural Drainage Networks: New Challenges from Structure-from-Motion Photogrammetry for Post-event Analysis." *Earth Surface Processes and Landforms*, Vol. 40, No. doi:10.1002/esp.3767.

Robson, B.A., Nuth, C., Dahl, S.O., Hölbling, D., Strozzi, T., and Nielson, P.R. (2015). "Automated Classification of Debris-Covered Glaciers Combining Optical, SAR and Topographic Data in an Object-Based Environment." *Remote Sensing of Environment*, Vol. 170, pp. 372-387. doi:10.1016/j.rse.2015.10.001.

Rosenblad, B.L., Gomez, F., Loehr, J.E., Gilliam, J. (2016). "Observations of Rockfall And Earth Slope Movements Using Ground-Based Interferometric Radar." *Proceedings 67th Highway Geology Symposium*, Colorado Springs, Colorado, USA.

Rosenblad, B.L., Gomez, F., Loehr, J.E., Legarsky, J., Jenkins, W. (2013). "Ground-Based Interferometric Radar for Monitoring Slopes and Embankments." *Proceedings Geo-Congress 2013*, San Diego, California, USA.

Scaioni, M., Longoni, L., Melillo, V., and Papini, M. (2016). "Remote Sensing for Landslide Investigations: An Overview of Recent Achievements and Perspectives." *Remote Sensing*, Vol. 6, No. 10, pp. 9600–9652. doi:10.3390/rs6109600.

Schild, K.M., Hawley, R.L., Chipman, J.W., Benn, D.I. (2017). "Quantifying Suspended Sediment Concentration in Subglacial Sediment Plumes Discharging from Two Svalbard Tidewater Glaciers Using Landsat-8 and In Situ Measurements." *International Journal of Remote Sensing*, Vol. 38, No. 23, pp. 6865–6881. doi:10.1080/01431161.2017.1365388.

Simmons, S.M., Parsons, D.R., Best, J.L., Orfeo, O., Lane, S.N., Kostaschuk, R., Hardy,

R.J., West, G., Malzone, C., Marcus, J., and Pocwiardowski, P. (2010). "Monitoring Suspended Sediment Dynamics Using MBES." *Journal of Hydraulic Engineering*, Vol. 136, No. 1, pp. 45–49. doi:10.1061/(ASCE)HY.1943-7900.0000110.

Sovilla, B. (2004). "Field Experiments and Numerical Modelling of Mass Entrainment And Deposition Processes in Snow Avalanches." Ph.D. dissertation, ETH Zürich, Zürich, Switzerland. doi:10.3929/ethz-a-004784844.

Sovilla, B., Burlando, P., and Bartelt, P. (2006). "Field Experiments and Numerical Modeling of Mass Entrainment in Snow Avalanches." *Journal of Geophysical Research*, Vol. 111, No. F3, pp. 1-16. doi:10.1029/2005JF000391.

Sovilla, B., McElwaine, J.N., Schaer, M., and Vallet, J. (2010). "Variation of Deposition Depth with Slope Angle in Snow Avalanches: Measurements from Vallée de la Sionne." *Journal of Geophysical Research*, Vol. 115, No. F2, pp. 1–13. doi:10.1029/2009JF001390.

Sovilla, B., Sommavilla, F., and Tomaselli, A. (2001). "Measurements of Mass Balance In Dense Snow Avalanche Events." *Annals of Glaciology*, Vol. 32, pp. 230–236.

Strozzi, T., and Ambrosi, C. (2007). "SAR Interferometric Point Target Analysis and Interpretation of Aerial Photographs for Landslides Investigations in Ticino, Southern Switzerland." *Proceedings Envisat Symposium 2007*, Montreux, Switzerland.

Strozzi, T., Ambrosi, C., and Raetzo, H. (2013). "Interpretation of Aerial Photographs And Satellite SAR Interferometry for the Inventory of Landslides." *Remote Sensing*, Vol. 5, No. 5, pp. 2554-2570. doi:10.3390/rs5052554.

Strozzi, T., Raetzo, H., Wegmüller, U., Papke, J., Caduff, R., Werner, C., and Wiesmann, A. (2015)." *Engineering Geology for Society and Territory*, Vol. 5, pp. 161–165. doi:10.1007/978-3-319-09048-1_32.

Tamminga, A. (2016). "UAV-Based Remote Sensing of Fluvial Hydrogeomorphology And Aquatic Habitat Dynamics." PhD dissertation, The University of British Columbia, Vancouver, BC, Canada.

Tamminga, A., Hugenholtz, C., Eaton, B., LaPointe, M. (2015). "Hyperspatial Remote Sensing of Channel Reach Morphology and Hydraulic Fish Habitat Using Unmanned Aerial Vehicle (UAV): A First Assessment in the Context of River Research and Management." *River Research and Applications*, Vol. 31, pp. 379–391.

Thatcher, C.A., Brock, J.C., Danielson, J.J., Poppenga, S.K., Gesch, D.B., Palaseanu-Lovejoy, M.E., Barras, J.A., Evans, G.A., and Gibbs, A.E. (2016). "Creating a Coastal National Elevation Database (CoNED) for Science and Conservation Applications." *Journal of Coastal Research*, Vol. 76, pp. 64–74. doi:10.2112/SI76-007.

Theler, D., Reynard, E., Bardou, E. (2008). "Assessing sediment dynamics from geomorphological maps: Bruchi torrential system, Swiss Alps", *Journal of Maps*, 4(1), https://doi.org/10.4113/jom.2008.1013.

Theler, D., Reynard, E., Lambiel, C., and Bardou, E. (2010). "The Contribution of Geomorphological Mapping to Sediment Transfer Evaluation in Small Alpine Cathments." *Geomorphology*, Vol. 124, pp. 113–123. doi:10.1016/j.geomorph.2010.03.006.

Thieler, E.R., Himmelstoss, E.A., Zichichi, J.L., and Ayhan, E. (2017). "Digital Shoreline Analysis System (DSAS) Version 4.0 - An ArcGIS Extension for Calculating Shoreline Change (ver. 4.4, July 2017): U.S. Geological Survey Open-File Report 2008–1278: https://woodshole.er.usgs.gov/project-pages/DSAS.

Torresan, C., Berton, A., Carotenuto, F., Di Gennaro, S.F., Gioli, B., Matese, A., Miglietta, F., Vagnoli, C., Zaldei, A., and Wallace, L. (2017). "Forestry Applications of UAVs in Europe: A Review." *International Journal of Remote Sensing*, Vol. 38, pp. 2427–2447. doi:10.1080/01431161.2016.1252477.

Turner, D., Lucieer, A., and De Jong, S. M. (2015). "Time Series Analysis of Landslide Dynamics Using an Unmanned Aerial Vehicle (UAV)." *Remote Sensing*, Vol. 7, No. 2, pp. 1736–1757.

Turner, D., Lucieer, A., and Wallace, L. (2014). "Direct Georeferencing of Ultrahigh-Resolution UAV Imagery." *IEEE Trans. Geoscience and Remote Sensing,*

Vol. 52, pp. 2738–2745.

Vriend, N.M., McElwaine, J.N., Sovilla, B., Keylock, C.J., Ash, M., and Brennan, P.V. (2013). "High-resolution Radar Measurements of Snow Avalanches." *Geophysical Research Letters*, Vol. 40, No. 4, pp. 727–731. doi:10.1002/grl.50134.

Wagner, W. (1998). "Soil Moisture Retrieval from ERS Scatterometer Data." PhD Dissertation, Vienna University of Technology.

Wang, J. and Stewart, R. (2015). "Inferring Marine Sediment Type Using Chirp Sonar Data: Atlantis Field, Gulf of Mexico. *Society of Exploration Geophysicists Technical Program Expanded Abstracts 2015*, pp. 2385–2390. doi:10.1190/segam2015-5918190.1.

Wegmüller, U. (1997). "Soil Moisture Monitoring with ERS SAR Interferometry." European Space Agency Special Publication ESA SP-414. *Proceedings 3rd ERS Symposium*, pp. 47–51.

Wegmüller, U., Strozzi, T., Delaloye, R., and Raetzo, H. (2012). "Landslide Mapping in Switzerland with Envisat ASAR." *Proceeding IGARSS 2012*, July 22–27, Munich, Germany.

Westoby, M. J., Brasington, J., Glasser, N. F., Hambrey, M. J., & Reynolds, J. M. (2012). "'Structure-from-Motion' Photogrammetry: A Low-cost, Effective Tool for Geoscience Applications." *Geomorphology*, Vol. 179, pp. 300–314.

Westoby, M. J., Dunning, S. A., Woodward, J., Hein, A. S., Marrero, S. M., Winter, K., Sugden, D. E. (2015). "Sedimentological Characterization of Antarctic Moraines Using UAVs and Structure-from-Motion Photogrammetry." *Journal of Glaciology*, Vol. 61, No. 230, pp. 1088–1102.

Wiesmann, A., Caduff, R., and Mätzler, C. (2015). "Terrestrial Radar Observations of Dynamic Changes in Alpine Snow." *IEEE Journal of Selected Topics in Applied Earth Observations and Remote Sensing*, Vol. 8, No. 7, pp. 3665–3671. doi:10.1109/JSTARS.2015.2400972.

Woodget, A.S. and Austrums, R. (2017). "Subaerial Gravel Size Measurement Using Topographic Data Derived from a UAV-SfM Approach." *Earth Surface Processes and Landforms*, Vol. 42, No. 9, pp. 1434–1443.

Kontroll- og referanseside/ Review and reference page

Dokumentinformasjon/*Document information*		
Dokumenttittel/*Document title* Remote Identification, Characterization and Monitoring of Erosional Processes		**Dokumentnr./*Document no.*** 20170031-03-R
Dokumenttype/*Type of document* Rapport / Report	**Oppdragsgiver/*Client*** NGI / NFR	**Dato/*Date*** 2018-03-21
Rettigheter til dokumentet iht kontrakt/ *Proprietary rights to the document according to contract* NGI		**Rev.nr.&dato/*Rev.no.&date*** 0 /
Distribusjon/*Distribution* ÅPEN: Skal tilgjengeliggjøres i åpent arkiv (BRAGE) / OPEN: To be published in open archives (BRAGE)		
Emneord/*Keywords*		

Stedfesting/*Geographical information*	
Land, fylke/*Country*	**Havområde/*Offshore area***
Kommune/*Municipality*	**Feltnavn/*Field name***
Sted/*Location*	**Sted/*Location***
Kartblad/*Map*	**Felt, blokknr./*Field, Block No.***
UTM-koordinater/*UTM-coordinates* **Zone: East: North:**	**Koordinater/*Coordinates*** **Projection, datum: East: North:**

Dokumentkontroll/*Document control*
Kvalitetssikring i henhold til/*Quality assurance according to NS-EN ISO9001*

Rev/ *Rev.*	**Revisjonsgrunnlag/*Reason for revision***	**Egenkontroll av/ *Self review by:***	**Sidemanns-kontroll av/ *Colleague review by:***	**Uavhengig kontroll av/ *Independent review by*:**	**Tverrfaglig kontroll av/ *Interdisciplinary review by:***
0	Original document	2018-03-15 Sean Salazar	2018-03-20 Regula Frauenfelder		

Dokument godkjent for utsendelse/ *Document approved for release*	**Dato/*Date***	**Prosjektleder/*Project Manager***
	21 March 2018	Unni Eidsvig

NGI (Norwegian Geotechnical Institute) is a leading international centre for research and consulting within the geosciences. NGI develops optimum solutions for society and offers expertise on the behaviour of soil, rock and snow and their interaction with the natural and built environment.

NGI works within the following sectors: Offshore energy – Building, Construction and Transportation – Natural Hazards – Environmental Engineering.

NGI is a private foundation with office and laboratories in Oslo, a branch office in Trondheim and daughter companies in Houston, Texas, USA and in Perth, Western Australia

www.ngi.no

NGI (Norges Geotekniske Institutt) er et internasjonalt ledende senter for forskning og rådgivning innen ingeniørrelaterte geofag. Vi tilbyr ekspertise om jord, berg og snø og deres påvirkning på miljøet, konstruksjoner og anlegg, og hvordan jord og berg kan benyttes som byggegrunn og byggemateriale.

Vi arbeider i følgende markeder: Offshore energi – Bygg, anlegg og samferdsel – Naturfare – Miljøteknologi.

NGI er en privat næringsdrivende stiftelse med kontor og laboratorier i Oslo, avdelingskontor i Trondheim og datterselskaper i Houston, Texas, USA og i Perth, Western Australia.

www.ngi.no

NGI
OSLO
TRONDHEIM
HOUSTON
PERTH

NORWEGIAN GEOTECHNICAL INSTITUTE
NGI.NO

Main office
PO Box 3930 Ullevaal St.
NO-0806 Oslo
Norway

Trondheim office
PO Box 5687 Torgarden
NO-7485 Trondheim
Norway

T (+47)22 02 30 00
F (+47)22 23 04 48
NGI@ngi.no

BIC NO. DNBANOKK
IBAN NO26 5096 0501 281
ORGANISATION NO.
958 254 318MVA

ISO 9001/14001
CERTIFIED BY BSI
FS 32989/EMS 612006